

Highly Coherent Electronically Tunable Waveguide Extended Cavity Diode Laser

Vincent Crozatier, Bijoy Krishna Das, Ghaya Baïli, Guillaume Gorju, Fabien Bretenaker, Jean-Louis Le Gouët, Ivan Lorgeré, and Wolfgang Sohler

Abstract—A frequency agile extended cavity diode laser using an integrated Bragg reflector in a Ti:Fe:LiNbO₃ waveguide is developed and characterized. The laser emits up to 7 mW in the 1.5- μm telecommunication window. The emission spectrum exhibits a 18-kHz linewidth, >40-dB sidemode suppression ratio, and a wavelength stability of ± 1 pm over hours. Very fast mode hop-free frequency tuning is achieved through the electrooptic effect, with a tuning slope of 55.5 MHz/V.

Index Terms—Integrated optoelectronics, laser tuning, LiNbO₃ waveguide, photorefractive grating, semiconductor laser.

HIGHLY coherent lasers emitting a stable frequency and capable of fast frequency scans over a limited range (typically 10 GHz in 10 μs) are required for several applications, for instance coherent transmission systems, LIDAR detection, modulation spectroscopy technique [1], optical frequency domain reflectometry [2], and RF signal processing [3]. In the last decade, several tunable semiconductor-based architectures have been proposed and developed. These include distributed feedback and distributed Bragg reflector semiconductor structures. Such devices are very compact, but their small size implies a megahertz linewidth. Moreover, the frequency sweeps are neither linear nor reproducible because of the interplay of electrical and thermal effects. Extended cavity diode lasers (ECDLs) using a diffraction grating exhibit narrower linewidths as well as good tunability, and can also be made very compact [4]. Wide tuning can be achieved by control of the grating displacement. However, very fast and precise frequency scans exclude mechanical movements and electrooptic (EO) effect is preferred to achieve such performances. Several cavities using an EO crystal have been proposed [5], [6]. They all feature linear and fast tuning capability over the required 10-GHz range, but the major issue remains in the high voltage needed, limiting both the scan range and speed. Moreover, the different elements constituting the cavity (diode, EO crystal, grating) make it very sensitive to external perturbations, hence degrading laser stability.

Better intrinsic stability can be achieved by integrating for example the EO phase section and the grating in a single device.

Manuscript received November 21, 2005; revised May 20, 2006. This work was supported in part by the Programme Nanosciences, Project LASCOH, and in part by the Deutsche Forschungsgemeinschaft (DFG) within the frame of the research unit "Integrated Optics in Lithium Niobate."

V. Crozatier, G. Gorju, F. Bretenaker, J.-L. Le Gouët, and I. Lorgeré are with the Laboratoire Aimé Cotton, CNRS, F-91405 Orsay CEDEX, France (e-mail: vincent.crozatier@lac.u-psud.fr).

B. K. Das and W. Sohler are with Angewandte Physik, Universität-GH Paderborn, D-33098 Paderborn, Germany.

G. Baïli is with the Laboratoire Aimé Cotton, CNRS, F-91405 Orsay CEDEX, France, and also with Thales Research and Technology, F-91767 Palaiseau CEDEX, France.

Digital Object Identifier 10.1109/LPT.2006.877549

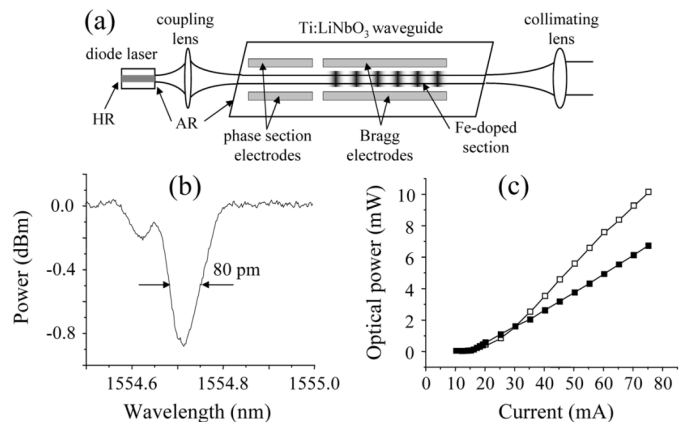


Fig. 1. (a) Principle of WECDL. (b) Bragg reflector transmission. (c) Optical power versus diode current. Empty squares: diode; filled squares: WECDL.

This can be done with an optical Bragg reflector integrated in a EO waveguide. Another advantage of integrated optics is the drastic reduction of the voltage needed for frequency scans. Indeed, the EO tuning response varies as the inverse of the electrodes spacing, usually limited by the beam size. From a bulk ECDL to a waveguide architecture, the spot size typically drops from 1 mm down to 10 μm , thus lowering the voltage by two orders of magnitude. Such a cavity has been demonstrated in a KTP substrate [7], but no real advantage was highlighted, as the EO response is about the same as in [6]. In this letter, we demonstrate a waveguide extended cavity diode laser (WECDL) in a LiNbO₃ substrate, working at 1.5 μm , with a high EO tuning slope. We also investigate the laser performance, proving that this source is ideal for the applications mentioned above.

The cavity is sketched in Fig. 1(a). The active medium is a diode laser with a high reflection coating ($R > 70\%$) on one side, and an antireflection (AR) coating ($R < 0.05\%$) on the other side. With a 75-mA current, it delivers up to 10 mW of amplified spontaneous emission in a 100-nm-wide spectrum [see Fig. 2(a)]. The far-field pattern is almost circular with a $\sim 40^\circ$ divergence angle. We couple the light into the waveguide using an AR-coated aspheric lens, driven by a three axis translation stage. Different waveguide structures delineated along the Z -axis are fabricated by photolithographically defined titanium indiffusion in the surface of an X -cut LiNbO₃ crystal. The substrate is 4.8 cm long, 1 mm thick, with end faces polished under an angle of 5.8° . The input face is AR-coated. The Ti stripes are 100 nm thick and their widths are either 14 μm (for two-mode guiding) or 7 μm (for single-mode guiding). The mode size of a single-mode waveguide is $\sim 7.5 \times 5.0 \mu\text{m}^2$ ($1/e^2$ values), approximately optimized for maximum light coupling to a standard single-mode fiber.

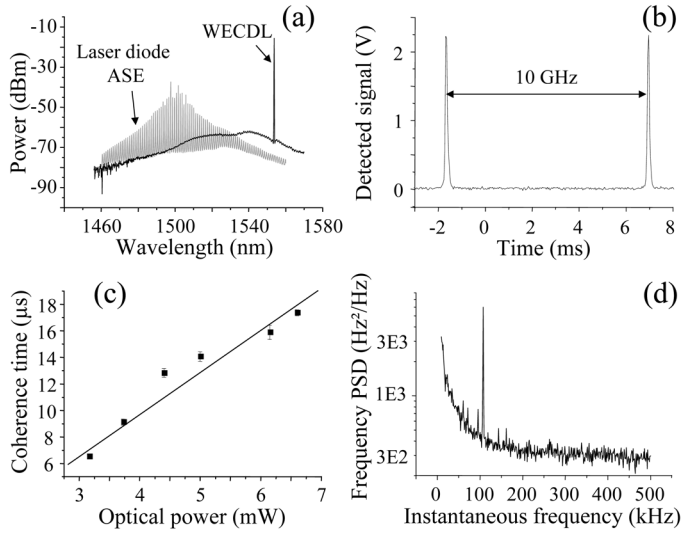


Fig. 2. (a) Optical spectrum of diode spontaneous emission (gray line) and WECDL (black line); (b) Fabry-Pérot spectrum. (c) Coherence time versus output power. Squares are experimental data and the solid line is linear fit. (d) Laser frequency PSD versus instantaneous frequency.

A 13-mm-long Bragg grating is engraved via photorefractive effect in a Fe-doped section of the waveguide by a holographic setup with an argon laser [8]. The grating is thermally fixed [8], [9] and later refreshed with blue light homogeneous illumination, using, e.g., GaN light-emitting diodes (LEDs). The Bragg reflectivity can be adjusted by the LEDs intensity. Fig. 1(b) shows a typical transmission spectrum of a Bragg grating, exhibiting a spectral width of 80 pm.

The throughput of the diode light in both single- and multi-mode waveguides reaches 60% in the absence of a grating. This includes the propagation losses of the waveguide, which are measured to be between 0.1 and 0.2 dB/cm. A Bragg reflectivity of about 20% and a diode current of 75 mA yields a 7-mW output power of the WECDL [see Fig. 1(c)] at 1553.75 nm. Single-frequency oscillation in a single spatial mode is obtained in the 14- μm -wide guides when the fundamental mode of the guide only is excited [see Fig. 2(b)]. In single-mode waveguides, the oscillation is single frequency at low current, but increasing the current leads to longitudinally multimode operation, and eventually coherence collapse. Single-frequency operation is also achieved in lossy single-mode waveguides. The reason for this observation remains unknown yet. The following characterization of laser operation is performed in a 14- μm guide. Relative intensity noise (RIN) measurements indicate a level of -145 dB/Hz on a cavity free spectral range (FSR), measured to be 2.1 GHz, and a 0.4% RIN standard deviation when integrated on a 0.1–20-GHz bandwidth. As for the polarization, the grating reflectivity is almost the same for both TE and TM polarizations. The only selective element is then the diode, which emits with a linear polarization along the crystal Y -axis (TE polarization).

We then investigate the spectral purity of our laser. Using a Fabry-Pérot interferometer, we measure a sidemode suppression ratio better than 40 dB. The suppression of the diode spontaneous emission is 50 dB, as can be seen in the optical spectrum analyzer trace of Fig. 2(a) (resolution 100 pm). We also

characterize the coherence time of our laser versus the injection current, with a self-heterodyne method. Results are shown in Fig. 2(c). The coherence time evolves almost linearly with the output power, exhibiting a maximum of 18 μs at 7 mW, which corresponds to a linewidth of 18 kHz.

Next, we estimate the laser stability on both short and long time scales. On the one hand, the laser jitter is measured using the technique developed in [10], with a fiber delay of 20 ns. The corresponding laser frequency power spectral density (PSD) is shown in Fig. 2(d). The technical noise (quasi- $1/f$ noise) is limited to a 100-kHz bandwidth only. The standard deviation associated to the PSD of Fig. 2(d) is 16 kHz in a 10–100-kHz integration bandwidth. As for long-term stability, the laser wavelength drifts within ± 1 pm, limited by the accuracy of our wavemeter, during hours without any external stabilization.

Finally, we test the frequency agility of the WECDL. Mode hop-free continuous tuning requires that the Bragg and the cavity mode wavelengths are simultaneously shifted at the same rate. Using two independent sets of electrodes, one located on the grating region, the other one on the phase section [see Fig. 1(a)], one can easily obtain this synchronization. Indeed, the Bragg frequency shift $\Delta\nu$ due to the voltage applied on the Bragg region V_B can be expressed as

$$\frac{\Delta\nu^{(\text{Bragg})}}{\nu} = \frac{\Delta n_{\text{eff}}}{n_{\text{eff}}} = -\frac{n_{\text{eff}}^2 r}{2d} \Gamma V_B \quad (1)$$

where n_{eff} is the effective refractive index, r the relevant EO coefficient, d the electrodes spacing, and Γ is the overlap of the electric field and the optical mode.

As for the phase variation, the frequency shift is expressed as follows:

$$\frac{\Delta\nu^{(\text{phase})}}{\nu} = \frac{\Delta L_{\text{cav}}}{L_{\text{cav}}} = -\frac{n_{\text{eff}}^3 r}{2d L_{\text{cav}}} \Gamma (L_{\phi} V_{\phi} + L_{B\text{eff}} V_B) \quad (2)$$

where L_{cav} is the cavity optical length, L_{ϕ} the phase electrode length. $L_{B\text{eff}} = \tanh(\kappa L_B)/(2\kappa)$ is the effective Bragg grating length, equal to half its physical length L_B in our case of low reflectivity ($\kappa L_B \ll 1$ with κ the coupling constant). This phase contribution from the Bragg grating is derived from the coupled mode theory [11].

Since the Bragg grating has to be fabricated along the Z -axis in order to exploit highest photovoltaic and EO effects in LiNbO_3 (coefficient $r_{33} = 30$ pm/V), we are limited to use the EO coefficient r_{22} (only 6 pm/V) for frequency tuning. The Bragg and phase section electrodes are 14 and 12 mm long, respectively. Considering $n_{\text{eff}} = 2.1$, $d = 14$ μm , and $\Gamma = 1$, we therefore expect the Bragg scale factor to be $K_B = 180$ MHz/V. As for the phase responses, we expect scale factors $K_{\phi} = 65$ MHz/V for the phase section and $K_{B\phi} = 38$ MHz/V for the Bragg section. These values are one order of magnitude higher as compared to bulk ECDLs [6]. Higher sensitivities would imply an X -cut/ Y -propagating or Y -cut/ X -propagating Z -polarized waveguide. This would also mean a lower Bragg reflectivity in the case of a photorefractive grating. However, Bragg gratings can be implemented with surface relief [12], [13] or proton exchange [14] techniques.

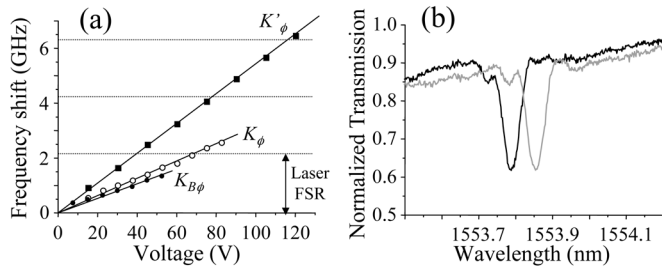


Fig. 3. (a) EO tuning of the Bragg section phase response (filled circles), the phase section (empty circles), and both sections with the same voltage (squares); solid lines are linear fits. (b) Bragg grating displacement with 120 V (gray line) and without voltage (black line).

As shown in Fig. 3, we experimentally measure the frequency shifts induced by the different sections. First, the phase section scale factor is $K_\phi = 32$ MHz/V [see empty circles in Fig. 3(a)]. The difference with the estimation of (2) must be attributed to two major points. First we considered $\Gamma = 1$, which is less in reality. Second, the relevant d value is not exactly the electrodes spacing but the electric field path, which is longer. As for the Bragg section response, we measure a scale factor $K_B = 69$ MHz/V [see Fig. 3(b)] and a phase response $K_{B\phi} = 22$ MHz/V [see filled circles in Fig. 3(a)]. These values have about the same relative error with respect to their estimates as K_ϕ . From experimental values of K_ϕ , $K_{B\phi}$, and L_ϕ , one computes $L_B = 16.5$ mm, which is in good agreement with the real length of 14 mm. Let us point out that the position of the Bragg electrodes relative to the Bragg grating is only approximate. Applying the same voltage on both sections, the laser frequency is linearly swept over 6.6 GHz, corresponding to a total EO scale factor of 55.5 MHz/V [see squares in Fig. 3(a)], which is consistent with $K_\phi + K_{B\phi} = 54$ MHz/V. Note that we did not exceed 120 V to prevent electrical damage of the waveguide. Although V_{phase} and V_{Bragg} are not balanced in this experiment, we observe mode hop-free tuning on more than three cavity FSRs as the difference between the frequency shifts induced by phase and Bragg sections remains lower than one FSR. Finally, let us mention that, although not optimized, the scale factor of 55.5 MHz/V is already larger than those reported in [6] and [7]. As discussed above, using the r_{33} EO coefficient instead of the r_{22} , the scale factor would rise to more than 250 MHz/V. The 10-GHz-wide frequency scans would, therefore, be achievable using conventional low-voltage electronics.

As the EO scale factor is enhanced in this architecture, one can produce multi-gigahertz-wide frequency sweeps using conventional electronics. This way, high-speed and wide-frequency scans are reachable. Indeed, we can scan 5.5 GHz in 5 μ s. The chirp purity is characterized using a beat note method [10]. The beat note frequency width is found to be a few percent of the beat frequency, meaning that the total error of the chirp is tens of megahertz. This value is not fully satisfactory, but due to the high scale factor, the laser is very sensitive to electrical noise, which is then converted into frequency jitter. The 100-mV noise of our amplifier corresponds to a 5-MHz spectral precision on the laser frequency. However, such technical problems can be overcome.

In conclusion, we demonstrated a high stability and high EO sensitivity WECDL working in the 1.5- μ m telecommunication window. The integrated optical cavity is composed by a tunable phase section followed by a tunable Bragg grating monolithically fabricated on the surface of an EO Ti:Fe:LiNbO₃ crystal. The laser emits up to 7 mW of optical power at 1553.75 nm, with a linewidth of 18 kHz and a sidemode suppression ratio larger than 40 dB. The technical noise is limited to a 100-kHz bandwidth and the long term drift is lower than 1 pm over hours. The laser frequency can be electrically tuned with a scale factor of 55.5 MHz/V over a spectral range of more than 6 GHz. Agility has been demonstrated with 5.5-GHz-wide scans in 5 μ s. Further work concerns single frequency operation in single-mode waveguides and studies on frequency agility so as to improve the chirp purity. We believe that this laser source corresponds to an ideal source for numerous applications and experiments.

ACKNOWLEDGMENT

The authors would like to thank E. Ducloux and C. Gagnol for assistance and discussions.

REFERENCES

- [1] C. L. Tang and J. M. Telle, "Laser modulation spectroscopy of solids," *J. Appl. Phys.*, vol. 45, no. 10, pp. 4503–4505, Oct. 1974.
- [2] W. Eickhoff and R. Ulrich, "Optical frequency domain reflectometry in single-mode fiber," *Appl. Phys. Lett.*, vol. 39, no. 9, pp. 693–695, Nov. 1981.
- [3] V. Crozatier, V. Lavielle, F. Bretenaker, J.-L. Le Gouët, and I. Lorgeré, "High-resolution radio frequency spectral analysis with photon echo chirp transform in an Er: YSO crystal," *IEEE J. Quantum Electron.*, vol. 40, no. 10, pp. 1450–1457, Oct. 2004.
- [4] A. Q. Liu, X. M. Zhang, D. Y. Tang, and C. Lu, "Tunable laser using micromachined grating with continuous wavelength tuning," *Appl. Phys. Lett.*, vol. 85, no. 17, pp. 3684–3686, Oct. 2004.
- [5] L. Ménager, L. Cabaret, and I. Lorgeré, "Diode laser extended cavity for broad-range fast ramping," *Opt. Lett.*, vol. 25, no. 17, pp. 1246–1248, Sep. 2000.
- [6] L. Levin, "Mode-hop-free electro-optically tuned diode laser," *Opt. Lett.*, vol. 27, no. 4, pp. 237–239, Feb. 2002.
- [7] K. Repasky, J. D. Williams, J. L. Carlsten, E. J. Noonan, and G. W. Switzer, "Tunable external-cavity diode laser based on integrated waveguide structures," *Opt. Eng.*, vol. 42, no. 8, pp. 2229–2234, Aug. 2003.
- [8] B. K. Das, H. Suche, and W. Sohler, "Single-frequency Ti:Er:LiNbO₃ distributed Bragg reflector waveguide laser with thermally fixed photorefractive cavity," *Appl. Phys. B*, vol. 73, no. 5–6, pp. 439–442, Oct. 2001.
- [9] C. Becker, A. Greiner, T. Oesselke, A. Pape, W. Sohler, and H. Suche, "Integrated optical Ti:Er:LiNbO₃ distributed reflector laser with a fixed photorefractive grating," *Opt. Lett.*, vol. 23, no. 15, pp. 1194–1196, Aug. 1998.
- [10] G. Gorju, V. Crozatier, V. Lavielle, I. Lorgeré, J.-L. Le Gouët, and F. Bretenaker, "Experimental investigation of deterministic and stochastic frequency noises of a rapidly frequency chirped laser," *Eur. Phys. J. Appl. Phys.*, vol. 30, no. 3, pp. 175–183, Jun. 2005.
- [11] A. Yariv, "Coupled-mode theory for guided-wave optics," *IEEE J. Quantum Electron.*, vol. QE-9, no. 9, pp. 919–933, Sep. 1973.
- [12] K. Chen, J. Ihlemann, P. Simon, I. Baumann, and W. Sohler, "Generation of submicron surface gratings on LiNbO₃ by ultrashort UV laser pulses," *Appl. Phys. A*, vol. 65, no. 4–5, pp. 517–518, Oct. 1997.
- [13] B. Wu, P. L. Chu, H. Hu, and Z. Xiong, "UV-induced surface-relief gratings on LiNbO₃ channel waveguides," *IEEE J. Quantum Electron.*, vol. 35, no. 10, pp. 1369–1373, Oct. 1999.
- [14] B.-E. Benkelfat, R. Ferrière, B. Wacogne, and P. Mollier, "Technological implementation of Bragg grating reflectors in Ti:LiNbO₃ waveguides by proton exchange," *IEEE Photon. Technol. Lett.*, vol. 14, no. 10, pp. 1430–1432, Jun. 2002.